Molecular Systems Biology 5; Article number 300; doi:10.1038/msb.2009.61
Citation: *Molecular Systems Biology* 5:300

www.molecularsystemsbiology.com

molecular systems biology

REPORT

Control and signal processing by transcriptional interference

Antoine Buetti-Dinh[1], Rosemarie Ungricht[1], János Z Kelemen, Chetak Shetty, Prasuna Ratna and Attila Becskei*

Institute of Molecular Biology, University of Zurich, Zurich, Switzerland
[1] These authors contributed equally to this work
* Corresponding author. Institute of Molecular Biology, University of Zurich, Winterthurerstrasse 190, Zurich 8057, Switzerland.
Tel.: +41 44 635 3180; Fax: +41 44 635 6811; E-mail: attila.becskei@molbio.uzh.ch

Received 28.11.08; accepted 21.7.09

A transcriptional activator can suppress gene expression by interfering with transcription initiated by another activator. Transcriptional interference has been increasingly recognized as a regulatory mechanism of gene expression. The signals received by the two antagonistically acting activators are combined by the polymerase trafficking along the DNA. We have designed a dual-control genetic system in yeast to explore this antagonism systematically. Antagonism by an upstream activator bears the hallmarks of competitive inhibition, whereas a downstream activator inhibits gene expression non-competitively. When gene expression is induced weakly, the antagonistic activator can have a positive effect and can even trigger paradoxical activation. Equilibrium and non-equilibrium models of transcription shed light on the mechanism by which interference converts signals, and reveals that self-antagonism of activators imitates the behavior of feed-forward loops. Indeed, a synthetic circuit generates a bell-shaped response, so that the induction of expression is limited to a narrow range of the input signal. The identification of conserved regulatory principles of interference will help to predict the transcriptional response of genes in their genomic context.
Molecular Systems Biology **5:** 300; published online 18 August 2009; doi:10.1038/msb.2009.61
Subject Categories: synthetic biology; chromatin & transcription
Keywords: noncoding transcription; promoter; repression

Introduction

One of the major goals of quantitative modeling of gene regulation is to predict gene expression based on the occupancy of gene regulatory sites by transcriptional factors. The action of transcriptional activators and repressors bound to a promoter can be represented as a mathematical operation. These operations have been systematically analyzed in prokaryotes (Buchler *et al*, 2003; Hermsen *et al*, 2006; Cox *et al*, 2007), and in eukaryotes (Ratna *et al*, 2009).

The above models focused on the classical role of transcriptional activators: the enhancement of gene expression. Interestingly, activators can also suppress gene expression by, at least, two different mechanisms (Shearwin *et al*, 2005).

First, intergenic transcription initiated by activators from upstream sequences can interfere with the expression of downstream genes. This upstream interference has been observed for the *SER3*, *ADH1* and *ADH3* genes in yeast (Martens *et al*, 2004, 2005; Bird *et al*, 2006). Intergenic transcription produces noncoding RNAs that have been detected in *Saccharomyces cerevisiae* and higher eukaryotes in large numbers (Hongay *et al*, 2006; Khaitovich *et al*, 2006; Neil *et al*, 2009; Xu *et al*, 2009). Positive regulatory aspects of transcriptional interference have been increasingly recognized in processes and phenomena, such as T-cell receptor recombination, latency of the HIV infection and epigenetic cellular memory (Schmitt *et al*, 2005; Abarrategui and Krangel, 2007; Lenasi *et al*, 2008).

Second, when an activator binds to a site that overlaps or is positioned downstream of the transcriptional initiation site, it can interfere with transcriptional initiation and elongation. This downstream antagonism is exemplified by the *ZRT2*, *PRY3* and *ACC1* genes (Li and Johnston, 2001; Bird *et al*, 2004; Bickel and Morris, 2006).

Signals passed onto transcriptional activators that either interfere with transcriptional initiation or initiate intergenic

transcription are processed 'horizontally' along the DNA, which is mediated predominantly by the polymerase. Little is known about how these antagonistic signals are combined. Using the yeast, *Saccharomyces cerevisiae*, as a eukaryotic model organism, we have explored the principles of this signal conversion and how these signals can be utilized to control gene expression.

Results and discussion

Competitive inhibition by upstream interference

We studied upstream transcriptional interference using chromosomally integrated gene constructs. In these constructs, intergenic transcription interferes with the expression of a downstream *GFP* reporter gene under the control of different promoters (Figure 1, Materials and methods section). The intergenic transcription was triggered by the transcriptional activator GEV, activity of which was modulated by estradiol. First, we used the *ADH1* promoter, which has been already shown to be regulated by interference at its original genomic locus (Bird *et al*, 2006). On activation of GEV using estradiol, the GFP expression driven by the *ADH1* promoter decreased in a graded way, so that the expression had a unimodal distribution in the cell population (Figure 1A, Supplementary Figure S8). Thus, the mean expression level can be adequately used to quantify the output of the system.

Next, we measured the changes in the mean GFP expression as the occupancy of the activator-binding sites within a downstream promoter was varied. For this purpose, doxycycline was used to modulate the binding of the transcriptional activator, rtTA, to two *tet* operators within the downstream promoter. The doxycycline-induced binding of rtTA to the promoter led to GFP expression (Figure 1B). We observed that the suppression of GFP expression by intergenic transcription was gradually relieved as the rtTA binding strengthened, when

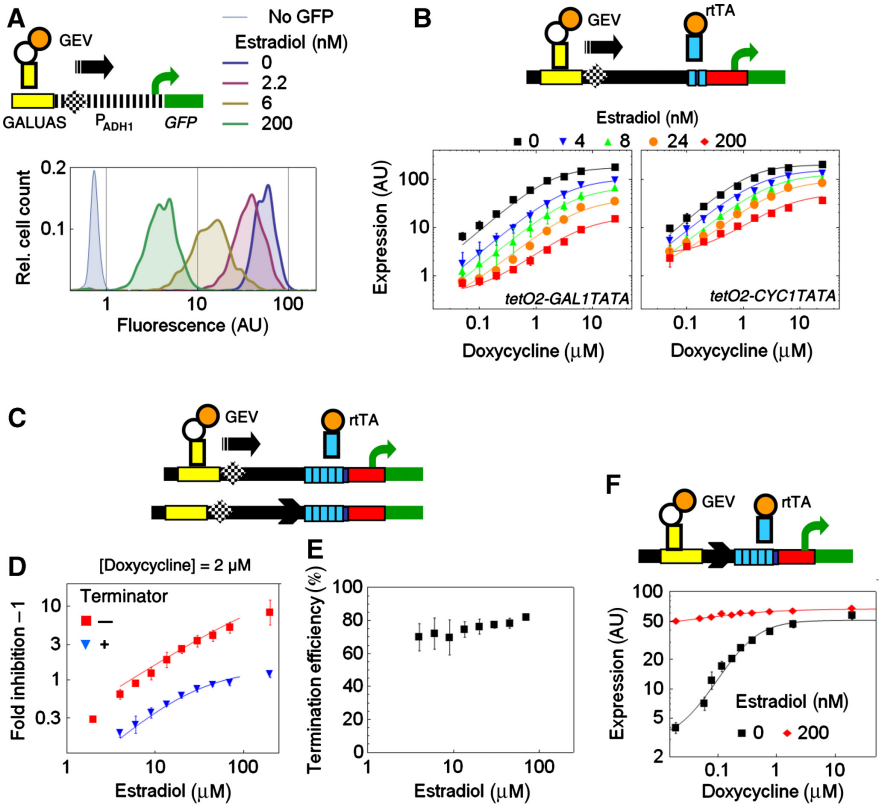

Figure 1 Upstream interference by intergenic transcription. (**A**) The 1000-bp long P_{ADH1} includes an upstream TATA box (−936 bp, checkered diamond), which is required to drive the intergenic transcription. Single cell distribution of *GFP* expression driven by *GALUAS*-$P_{ADH1(-1000\ to\ -1)}$ (YAntH44.6) is shown when intergenic transcription was activated at different estradiol concentrations. Relative cell count is shown. (**B**) The upstream activating sequence (UAS) of *GAL1*, *GALUAS*, was positioned upstream of the truncated *EGT2* gene (*EGT2* −115 to 509) to emulate intergenic transcription. The truncated gene comprises the core promoter with a TATA box (−115 to 0) and part of the ORF (1–509). The downstream promoter was obtained by fusing the $[tetO]_2$ to the *GAL1* or *CYC1* core promoters including a TATA box (YABH39.4 and −38.2). Expression was induced by doxycycline at different fixed concentrations of estradiol. Error bars represent s.d. values calculated from three experiments. The curves represent fits of the non-equilibrium model of upstream interference (see Supplementary Information), with α=3, k_{ON}=0.015 nM^{-1} min^{-1}; k_b=1 min^{-1}, η=49.6, k_r=0.041 min^{-1}, k_S=10 min^{-1}, m=33.4. A_{tot}=9.9 nM and K_{ind}=6.1 to account for the induction by doxycycline, and P=0, 1.5, 3.5, 8.6 and 71 for the respective estradiol concentrations. k_{OFF}=0.11 min^{-1}, β=2.8, *bas*=0.0055, v_{max}=201 for $P_{[tetO]2\text{-}GAL1TATA}$; and k_{OFF}=0.07 min^{-1}, β=7, *bas*=0.03, and v_{max}=230 for $P_{[tetO]2\text{-}CYC1TATA}$. (**C**) Constructs used to measure termination efficiency. The arrowhead denotes the *ACT1* transcriptional terminator. The downstream promoter was obtained by inserting five *tet* operators into the *EGT2* promoter. (**D**) Expression was induced by 2 μM doxycycline and was inhibited by increasing concentrations of estradiol. Data are shown for *GALUAS-EGT2*(−115 to 509)-$P_{[tetO]5inEGT2}$ (YAntH41.1, red squares) and *GALUAS-EGT2*(−115 to 509)- T_{ACT1}–$P_{[tetO]5inEGT2}$ (YAntH42.1, blue triangles). (**E**) The termination efficiency was calculated from two independent experiments (see Materials and methods section) using the data as shown in (D). (**F**) Activation of gene expression by GEV when only the T_{ACT1} separates the *GALUAS* from $P_{[tetO]5inEGT2}$ (YAntH43.1). Source data is available for this figure at www.nature.com/msb.

the doxycycline concentration was increased from intermediate to high levels (Figures 1B and 2B). This indicates that intergenic transcription competes with the rtTA-driven transcription.

We compared the expression data obtained at different strengths of intergenic transcription with basic equilibrium models of repression (Box 1). The data agreed well with the model of competitive inhibition, at weak and moderate intergenic transcription (Figure 2A and B). The drop of inhibition efficiency close to saturation of activator-binding sites, a hallmark of competitive inhibition, was particularly pronounced with a promoter containing seven operators (Figure 2C and Supplementary Figure S9C and D), in which a higher degree of operator occupancy can be attained due to cooperative binding of rtTA (Becskei *et al*, 2005). The overwhelming majority of the data points aligned closely with the fitted curves calculated from the equilibrium competition model (Figure 2C).

The equilibrium competition model did not fit the data when interference was strong (Supplementary Figure S10). In this case, a good fit was obtained only to the data points measured at high concentration of doxycycline (Figure 2B and C). When these fits were extended into the range of low doxycycline concentrations, they overestimated the inhibition of gene expression, suggesting that intergenic transcription can have a positive effect on GFP expression (Figure 2B and C). To evaluate how general the above observations are, we studied interference when expression at the downstream promoter was driven by various activation domains (VP16 and Swi5) and by various core promoters (*CYC1*, *GAL1* and *EGT2*). In all the examined cases, the two hallmarks were conserved, and only the overall efficiency of inhibition varied (Supplementary Figure S12); the competition dominated at medium and high doxycycline concentrations, whereas the positive effect of strong intergenic transcription was unmasked at a low doxycycline concentration.

Next, we built a detailed model on the basis of realistic molecular mechanisms. Previous studies have suggested that competition by intergenic transcription can arise when the elongating polymerase occludes the activator-binding sites (Sneppen *et al*, 2005). Furthermore, the elongating polymerase roadblocked by the activator can exert a force on the activator–DNA complex and destabilize it, after which the activator dissociates (Prescott and Proudfoot, 2002; Mosrin-Huaman *et al*, 2004; Galburt *et al*, 2007). However, when the polymerase traverses binding sites within the promoter, they can become more accessible, possibly due to changes in the chromatin structure, which enables the facilitated rebinding of transcription factors to them (Uhler *et al*, 2007). It is important to note that different methods for measuring DNA–protein interactions can produce contrasting results for the binding of the same transcription factor, when exposed to intergenic transcription (Bird *et al*, 2006). We constructed a non-

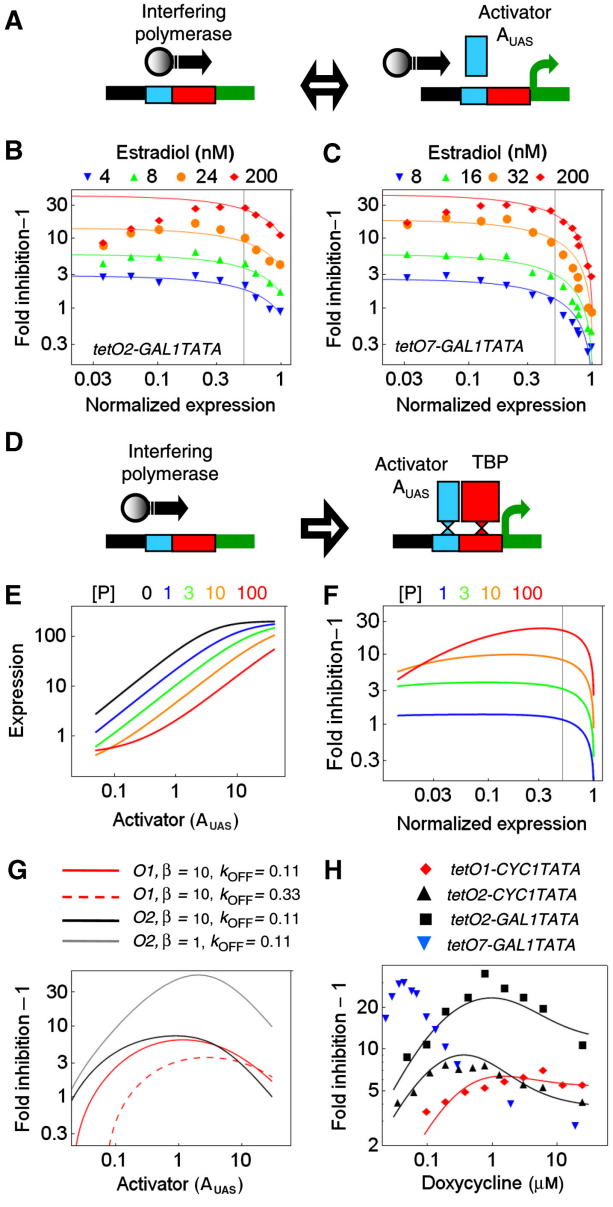

Figure 2 Equilibrium (**A**–**C**) and non-equilibrium competition models (**D**–**H**) of upstream interference. (A) Scheme of the equilibrium competition model. The downstream promoter is occupied either by the interfering polymerase or by the activator, A_{UAS}. (B, C) Equation (1) (Box 1) was fit to the data. K_D^A=0.37 and $f(R)$=2.9, 5.9, 14.1* and 41.4* for $P_{tetO2\text{-}GAL1TATA}$ (data re-plotted from Figure 1B) (B); K_D^A=0.024 and $f(R)$=2.6, 5.9, 18.5 and 42.7* for $P_{tetO7\text{-}GAL1TATA}$ (YABH34.5) (C). The asterisked $f(R)$ values were obtained by fitting equation (1) to data points that had a normalized expression higher than 0.4 (see Materials and methods section). (D) In the non-equilibrium competition model, the interfering polymerase traverses the UAS and the TATA box in the downstream promoter, after which they bind the activator, A_{UAS}, and the TBP with a higher affinity. (E) Gene expression as a function of A_{UAS} was calculated from the non-equilibrium model with the parameter values fitted for $P_{tetO2\text{-}GAL1TATA}$ (Figure 1B). The concentration of the activator [P] driving the intergenic transcription is color coded. (F) Curves were re-calculated from (E). (G) Fold inhibition at P=100 was calculated for promoters with one (O1) and two (O2) operators as in (F), except for the parameters specified in the figure legend. The red dashed line stands for one operator with reduced affinity. (H) Fold inhibition was measured at 200 nM estradiol as the doxycycline concentration was varied. The curves were fit with the parameter values obtained for the corresponding constructs in (Figure 1B). To link the A_{UAS} concentration to the doxycycline concentration, A_{tot}=10.3 nM and K_{ind}=2.6 were fit for promoters with CYC1TATA, measured on the same day. For $P_{tetO1\text{-}CYC1TATA}$ (YABH40.6), k_{ON}=0.0072 $nM^{-1}\,min^{-1}$ and k_{OFF}=0.13 min^{-1} were fitted to account for its lower binding constant in comparison with $P_{tetO2\text{-}CYC1TATA}$. Source data is available for this figure at www.nature.com/msb.

Box 1 Competitive and non-competitive inhibition of gene expression

Two basic forms of inhibition of gene expression are described by simple equilibrium models. When an inhibitor, R, interferes with the binding of the transcriptional activator, A, inhibition of gene expression is competitive. Expression is given by

$$\mathrm{Ex} = w\frac{A}{K_{\mathrm{D}}^{\mathrm{A}}(1+f(R))+A} \quad (1)$$

$K_{\mathrm{D}}^{\mathrm{A}}$ is the dissociation constant of the activator binding, w is a proportionality constant, whereas $f(R)$ is a lumped parameter incorporating the concentration and the dissociation constant of the inhibitor.

If the inhibitor does not prevent the activator from binding to the promoter, but suppresses transcription at a later stage, inhibition is non-competitive. A more general model incorporates the synergistic binding of the activator and the inhibitor, as well.

$$\mathrm{Ex} = w\frac{A}{K_{\mathrm{D}}^{\mathrm{A}}+A+K_{\mathrm{D}}^{\mathrm{A}}f(R)+\alpha A f(R)} \quad (2)$$

α denotes to what extent more likely is the joint binding of the activator and inhibitor than the binding assuming no interaction between them.

Characteristic profiles of inhibition, across a broad range of expression levels, can be conveniently compared when the fold change of expression due to a fixed concentration of the inhibitor is calculated as the activator concentration is varied. For this purpose, fold inhibition-1 was plotted against normalized expression (see Materials and methods section). Normalized expression, NE, corresponds to the expression, Ex, calculated in the absence of the inhibitor ($f(R)=0$, $w=1$ in equations (1 and 2)); $\mathrm{NE}=\mathrm{A}\cdot(K_{\mathrm{D}}^{\mathrm{A}}+\mathrm{A})^{-1}$.

Competitive inhibition is shown for $K_{\mathrm{D}}^{\mathrm{A}}=0.043$, $f(R)=3.8$ in equation (1).

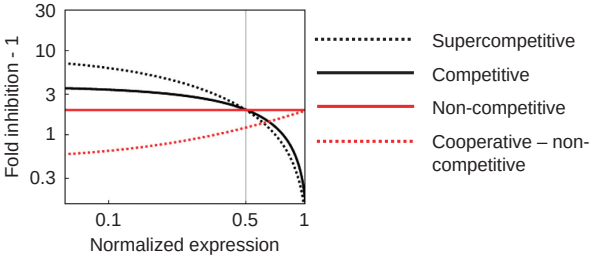

When gene expression approaches saturation, fold inhibition-1 drops rapidly, because the activator does not increase the expression noticeably but can increasingly outcompete R. However, fold inhibition-1 doubles at most, when the normalized expression is reduced from 0.5 to an arbitrary low value. For the supercompetitive mechanism, fold inhibition-1 increases more than twice when the normalized expression is reduced from 0.5 to an arbitrary low value. The supercompetitive curve is plotted for $K_{\mathrm{D}}^{\mathrm{A}}=0.043$, $f_1(R)=0$, $f_2(R)=0.1$ and $\alpha=0.011$ using equation (4) given by Ratna *et al*, 2009. Supercompetitive inhibition arises when the activator and the repressor jointly determine the permissive state of the promoter (Ratna *et al*, 2009).

For non-competitive inhibition, fold inhibition-1 has a constant value as transcriptional activation is varied (the curve is shown for $K_{\mathrm{D}}^{\mathrm{A}}=0.043$, $f(R)=2$ and $\alpha=1$ in equation (2)). When R and the activator bind cooperatively ($K_{\mathrm{D}}^{\mathrm{A}}=0.043$, $f(R)=0.5$ and $\alpha=4$ in equation (2)), fold inhibition-1 decreases with decreasing transcriptional activation (also see Supplementary Figure S3).

equilibrium model that includes the rebinding of rtTA facilitated by a factor of β, and the increased association of the TATA-binding protein (TBP) and the above forms of competition (Figure 2D, Supplementary Figure S1).

The model successfully reproduced the positive effect on gene expression while preserving the hallmarks of competition (Figure 2E and F, Supplementary Figure S2). The model fitted to data obtained for promoters containing two *tet* operators (Figure 1B) also predicts that the peak value of inhibition by intergenic transcription does not increase when the interfering polymerase competes with the rtTA bound to only one operator, or may even decrease if the single operator has a lower affinity (Figure 2G). Inhibition of expression caused by strong intergenic transcription reaches its peak value at intermediate doxycycline concentrations, at which intergenic transcription can more easily outcompete rtTA-induced transcription and the positive effect is still negligible. The above prediction was consistent with the measurements: the peak inhibition for the tetO1-CYC1TATA construct was lower, and shifted to higher doxycyline levels in comparison with the tetO2-CYC1TATA construct (Figure 2H, Supplementary Figure S11). Similarly, when the number of *tet* operators, fused to a GAL1 core promoter, was increased from two to seven, the inhibition curve only shifted towards lower doxycycline values but its peak value did not change (Figure 2H).

Initiation and termination of transcriptional interference

The prevalence of interference in the genomic context depends on the number of DNA sequences that can initiate interference, and on how efficiently transcriptional terminators terminate transcription between adjacent genes to prevent interference. With some modifications, the above gene constructs can shed light on how likely interference arises at a given segment of the genome (Supplementary Figure S13).

When two different activators bind to a promoter, both of them can activate gene expression (Supplementary Figure S13C). Surprisingly, the insertion of a short, eight-nucleotide long TATA sequence converts the activator recruited to a site upstream of the TATA box into an inhibitor of expression (Supplementary Figure S13B). This inhibition, triggered by a simple sequence, was less efficient than the inhibition by intergenic transcription initiated by a full promoter (Supplementary Figure S13A, B and D).

The efficiency of termination was extrapolated by measuring to what extent interference was reduced when a terminator was inserted between the intergenic transcription unit and the downstream promoter–GFP constructs (Figure 1C). The efficiency of termination was calculated at intermediate rtTA binding, when the inhibition of expression is linearly dependent on estradiol concentration (Figure 1D). The *ACT1* transcriptional terminator had a relatively constant, around 80%, termination efficiency over a broad range of intergenic transcription rates (Figure 1E). This constancy of the efficiency is surprising because it has been commonly assumed that terminators fail when the transcription rate passes a threshold value.

The genomes of yeast species are very compact and transcriptional terminators often overlap with the promoters of downstream genes (Valerius *et al*, 2002). Therefore, termination efficiency inferred from the changes in transcriptional interference is important to assess how efficiently terminators can isolate the transcriptional regulation of two adjacent genes.

Interestingly, the terminator did not reduce transcriptional activation when it was inserted directly downstream of a UAS that had no TATA box associated with it (Figure 1F). This suggests that terminators do not prevent an activator from initiating transcription at a TATA box positioned downstream of the terminator (Figure 1F), but they terminate transcription that had been fully initiated (Figure 1D).

Genome-wide analyses of gene expression suggest that genes may not reach their optimal expression level because of interference of their genomic environment (Liao and Zhang, 2008); and evolution proceeds in a direction to increase intergenic distances, whereby interference is reduced (Chiaromonte *et al*, 2003; Byrnes *et al*, 2006). Indeed, the simple DNA sequence requirements for the interference to be initiated (Supplementary Figure S13B) and, the good, but finite (~80%), efficiency of transcriptional termination between adjacent genes may contribute to the widespread occurrence of interference in the genome.

Downstream antagonism

To study antagonism by downstream activators, activator-binding sites were inserted downstream of the TATA box in the promoter–GFP constructs. Binding of GEV to the upstream site, GALUAS, drove the expression of GFP (Figure 3A). The binding of rtTA to *tet* operators downstream of a TATA box inhibited GFP expression (Figure 3A). This indicates that in addition to DNA-binding protein domains alone (Brent and Ptashne, 1984; Murphy *et al*, 2007), full-length transcriptional activators can interfere with the transcriptional activation. Expression data at different strengths of downstream antagonism were in excellent agreement with an equilibrium model for non-competitive inhibition that incorporates the cooperative binding of GEV and rtTA (Box 1, Figure 3A and B) (Cornish-Bowden, 2004). Cooperative binding of rtTA to promoters has been observed (Becskei *et al*, 2005). The cooperative interaction between the upstream and downstream sites could account for the observation that at a low estradiol concentra-

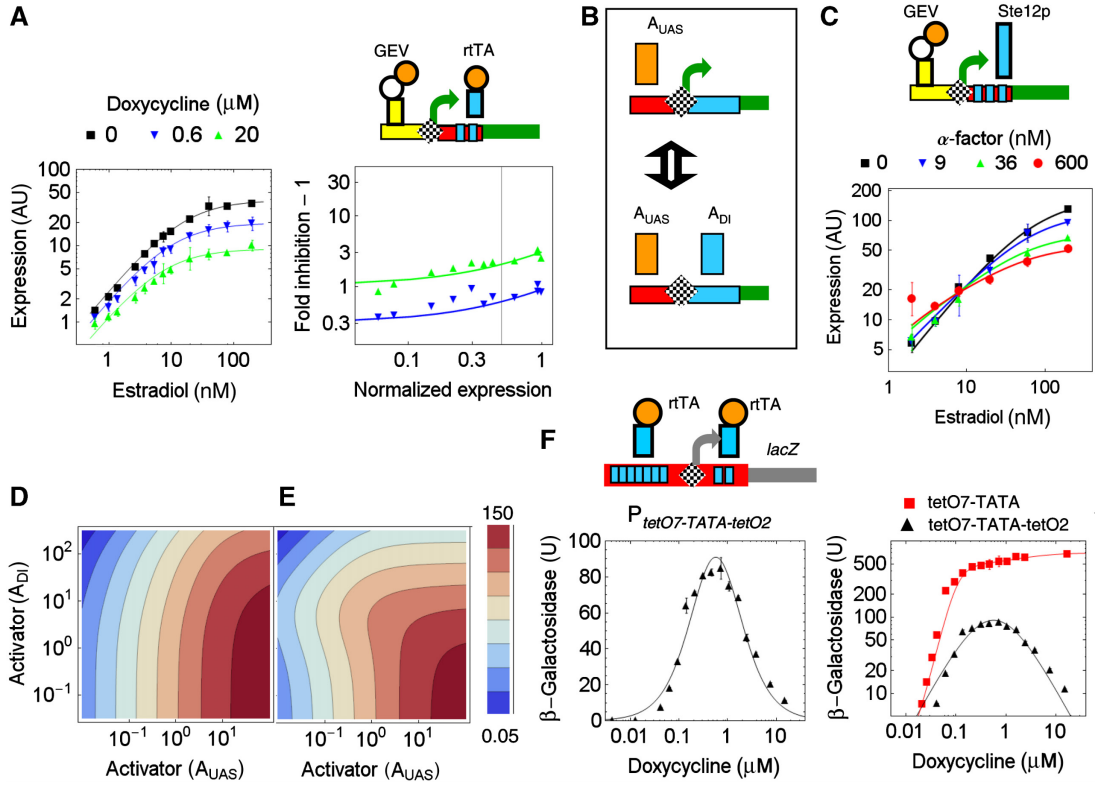

Figure 3 Downstream antagonism. The TATA box is denoted by a checkered diamond in the genetic constructs. Error bars represent s.d. values calculated from three experiments, unless otherwise specified. (**A**) Expression driven by $P_{GALUAS\text{-}TATA\text{-}tetO2}$ (RUY20) in the presence of different fixed concentrations of doxycycline. The curves were obtained by fitting equation (2) (Box 1): K_D^A=0.067, α=3.2. $f(R)$=0.31 and 1.05 for respective doxycycline concentrations (**B**) Scheme of non-competitive inhibition. When the A_{UAS} and A_{DI} activators bind to the promoter simultaneously, no transcription is initiated. (**C**) Expression driven by $P_{GALUAS\text{-}TATA\text{-}FUS1UAS}$ (YABH42.1) in the presence of different fixed concentrations of α-factor. The *FUS1UAS* contains three binding sites for the endogenous Ste12p transcriptional activator. Expression was adjusted using the $P_{GALUAS\text{-}TATA\text{-}MutFUS1UAS}$ construct (YABH43.2) to account for the nonspecific effects of α-factor on expression (see Materials and methods section). The curves are fits to the non-equilibrium model of the downstream antagonism (see Supplementary Information, SEq2) with p_{UAS}=0.01 nM^{-1} min^{-1}, p_{DI}=0.005 nM^{-1} min^{-1}, α=32.8, m_1=0.07 min^{-1}, m_2=0.1 min^{-1}, p_3=1 min^{-1}, m_3=0.2 min^{-1} and k=0.2 min^{-1}, A_{tot}=500 nM, K_{ind}=2161 nM, v_{max}=619; [A_{DI}]=0, 0.89, 2.79 and 4.46 for the respective α-factor concentrations. (**D**, **E**) Contour plots represent expression levels as a function of A_{DI} and A_{UAS} using the parameter values as in (C), except for p_{DI}=0.01 nM^{-1} min^{-1}, and the cooperativity of binding, α was varied: α=1 (D) and α=20 (E). (**F**) Expression driven by the $P_{tetO7\text{-}TATA\text{-}tetO2}$ (RUY65) and $P_{tetO7\text{-}CYC1TATA}$ (RUY67.13) constructs. LacZ was used to detect gene expression with higher sensitivity. Expression of the $P_{TATA\text{-}tetO2}$ construct (RUY69), which lacks an upstream activation sequence, is below the detection limit. The value for s.d. is calculated from two experiments. The bell-shaped curve was obtained by fitting SEq. 4 (w=470, n=m=1.2, N=0.46 and M=0.79). Source data is available for this figure at www.nature.com/msb.

tion, inhibition is weaker than predicted by a model of pure non-competitive inhibition.

To further explore the cooperative interaction between multiple binding events, three binding sites were inserted downstream of the TATA box, which are recognized by the Ste12p activator (Figure 3C). Ste12p activates its target genes when induced by α-factor, but it inhibits the expression of the *PRY3* gene by binding to a downstream site (Bickel and Morris, 2006). When the expression of the resulting $P_{GALUAS\text{-}TATA\text{-}FUS1UAS}$ construct was induced by high concentration of estradiol, addition of α-factor inhibited transcription in a dose-dependent manner (Figure 3C). However, at lower estradiol concentration, expression was paradoxically increased in response to increasing α-factor concentrations. This illustrates that interference in the same genetic construct can result in both inhibition and activation. Correspondingly, Ste12p buffers the action of GEV when induced by high concentration of α-factor, as expression changes only slightly over a broad range of estradiol concentrations.

The paradoxical activation can be explained when the above model was modified so that the activator bound to the downstream site induced a weak expression indirectly by a non-equilibrium kinetic effect on the upstream activator or directly by recruiting the transcription initiation machinery (Figures 3C and Supplementary Figures S4–S6).

Cooperative interactions are typically considered to be advantageous for regulation. For example, cooperative binding of repressors increases the sensitivity of response, making repression respond to environmental stimuli in a switch-like manner (Oehler *et al*, 2006). Thus, the reduction of inhibition by the cooperative interaction of the two antagonistic activators seems rather disadvantageous for regulation. However, a two-dimensional input plot reveals that the cooperativity renders the response more square-like, so that high expression is restricted to a quadratic domain in which the occupancy of the upstream sites is high and that of the downstream sites is low (compare Figure 3D and E).

A genome-wide search retrieved many activator-binding sites downstream of a TATA box that are conserved in related yeast species (Supplementary Table S1). Some of these sites may regulate gene expression. A Mac1p-binding site downstream of the TATA box of the *FTR1* promoter inhibited gene expression, and activated expression when transferred to an upstream site (Supplementary Figure S15). This finding may explain in part why the deletion of Mac1p, a copper-responsive transcriptional activator, results in an increase in *FTR1* expression (De Freitas *et al*, 2004).

In all the retrieved promoters (Supplementary Table S1), a single binding site downstream of the TATA box was identified. Therefore, downstream antagonism is expected to follow the non-competitive inhibition with cooperative binding (Figure 3A).

Bell-shaped response

Both the equilibrium and non-equilibrium models predict that binding of the same activator to both the upstream and downstream sites generates a bell-shaped response (Supplementary Figure S7). When rtTA binds to *tet* operators flanking the TATA box, increasing doxycycline concentration resulted in a bell-shaped response: expression initially increased and after reaching a plateau, it declined (Figure 3F, Supplementary Figure S16). The peak expression in the bell-shaped response is around five times less than the maximal expression of the corresponding expression cassette containing the upstream activation sequence only, confirming the predictions of the model. As the bell-shaped response limits gene expression to a narrow range of inducer concentrations it has the ability to translate concentration gradients into localized expression patterns, similar to the stripe formation during embryonic development (Sanchez and Thieffry, 2003; Basu *et al*, 2005). This response is reminiscent of the output of gene circuits with feed-forward loops (Mangan and Alon, 2003; Kaplan *et al*, 2008).

The regulatory architecture of the *ZRT2* promoter is very similar to our construct that generated bell-shaped response (Figure 3F). The Zap1p activator binds to sites flanking the TATA box of the *ZRT2* promoter. Although prior experiments have focused on repression by Zap1p, the full data set is compatible with a bell-shaped response to zinc (Supplementary Figure S17) (Bird *et al*, 2004). This similarity underscores the utility of studying signal processing by synthetic circuits to understand the functioning of natural gene networks.

Conclusions

It is essential to know to what extent gene expression can be inhibited as transcriptional activation is varied to understand gene regulation and to design gene expression systems for biotechnological purposes. Simple equilibrium models were consistent with most of our observations. In particular non-competitive inhibition with cooperative binding is consistent with the findings on downstream antagonism, including the bell-shaped response, which has been observed in the genomic context as well (Bird *et al*, 2004). The equilibrium approach is frequently used to describe gene regulation when transcription factors bind to promoters, because binding is a reversible process and rapid relative to the kinetics of the reporter gene expression. A more complex non-equilibrium model is realistic to explain interference, for which the regulator is transcription itself. Transcription is a highly irreversible process as the elongating polymerase proceeds only in one direction. This energy consuming interfering polymerase regulates the expression of the gene it traverses. Therefore, the non-equilibrium approach can capture the irreversible nature of processes having a function in upstream interference. Interestingly, intergenic transcription inhibits the expression at $P_{tetO2\text{-}CYC1TATA}$ less efficiently than at $P_{tetO2\text{-}GAL1TATA}$, even though rtTA has nearly equal affinities for these promoters (Figure 2B). The fitted non-equilibrium model suggests that rtTA rebinds and restores the initiation complex more rapidly at $P_{tetO2\text{-}CYC1TATA}$, after the polymerase traverses the promoter. This may explain why the expression at $P_{tetO2\text{-}CYC1TATA}$ is more resistant to interference.

Our findings reveal unexpected links between different forms of transcriptional regulation. Both upstream interference and classical repression by repressor proteins in yeast rely on competitive inhibition even though they represent distinct molecular mechanisms (Ratna *et al*, 2009). These simple

regulatory principles will help understand how genes generate complex responses in the genomic context.

Materials and methods

Genetic constructs

GEV is a fusion protein consisting of the Gal4p DNA binding domain, an estradiol receptor domain and the transcriptional activation domain, VP16-AD (Louvion *et al*, 1993). rtTA is a fusion of the rtetR DNA binding domain and the VP16-AD (Urlinger *et al*, 2000). The rtetR–(NLS-AD)^{Swi5} fusion was obtained by linking the following DNA sequences: rtetR(S2)(1–643), GGGCGCGCC, *SWI5*(1900–2125), CCTGCAGGG and *SWI5*(4–1639). rtTA(S2) served as a template for producing rtetR(S2). We used the enhanced green and the yellow variants of the green fluorescent protein as specified in Supplementary Table S2.

Yeast strains and growth conditions

All strains are congenic with W303 (*ade2-1*, *leu2-3*, *ura3*, *trp1-1*, *his3-11,15* and *can1-100*). Genetic constructs were integrated into the chromosome (Supplementary Table S3).

Cells containing inducible gene expression constructs were grown for 5 h after induction in minimal medium, until a cell density of OD_{600}=0.4–0.8, unless specified otherwise, was attained. When α-factor was added to cell culture at OD_{600}=0.025, cells were grown for 200 min.

Co-expression of GEV and rtTA did not affect the growth rate of the cells and the percentage of cells that lost the constructs containing the reporter gene and rtTA was $<0.01\,\%$ (Supplementary Figure S14).

β-Galactosidase assay

β-Galactosidase activity was measured using cell extracts obtained from freeze–thaw cycles and CPRG was used as a substrate.

Flow cytometry and calculation of expression

Total fluorescence of, at least, 5000 cells was measured using flow cytometry. About 5–15% of total cell population was selected in the forward-scatter versus side-scatter plot to measure GFP fluorescence of cells with similar size. To calculate expression (Ex), the total fluorescence of GFP expressing cells ($F_{e,d}$) was divided by the background fluorescence of a control strain (F_C), which expresses *lacZ* only:

$$Ex_{e,d} = \frac{F_{e,d}}{F_C} - 1$$

The e and d subscripts refer to the applied concentration of estradiol and doxycycline, respectively.

The α-factor causes changes in the forward and side scatter of the cells in a concentration-dependent manner, and also in the expression level induced by estradiol. The latter effect of α-factor may be caused directly by changes in general transcriptional rates and/or indirectly caused by changes in cell growth and consequently in dilution rate of GFP. Therefore, expression was corrected by the expression of a construct in which the Ste12p-binding sites were mutated (YABH43.2):

$$Ex_{e,\alpha} = \frac{\left(\frac{FW_{e,\alpha}}{C_\alpha} - 1\right)\left(\frac{FM_{e,0}}{C_0} - 1\right)}{\frac{FM_{e,\alpha}}{C_\alpha} - 1}$$

where C_0 and C_α denote the control cell fluorescence at zero and the applied α-factor concentration, respectively. $FW_{e,\alpha}$ and $FM_{e,\alpha}$ denote GFP fluorescence of constructs with wild-type and mutant Ste12p binding sites, respectively. $FM_{e,0}$ corresponds to $FM_{e,\alpha}$, when α=0.

The background expression is typically low and is subject to large relative fluctuations when exposed to interference, which makes it difficult to discern the effect of interference when gene expression is not induced (Supplementary Table S4).

Data analysis

Normalized expression, NE, is the uninhibited expression at a given degree of activation divided by the maximally induced expression:

$$NE_{0,d} = \frac{Ex_{0,d}}{Ex_{0,d_{max}}} \text{ for upstream interference}$$

$$NE_{e,0} = \frac{Ex_{e,0}}{Ex_{e_{max},0}} \text{ for downstream antagonism}$$

For upstream interference d_{max}=20 μM; for downstream antagonism e_{max}=200 nM. Fold inhibition at a given point of normalized expression was obtained by dividing expression in the absence of antagonism by the expression suppressed by the antagonistic activator:

$$FI_{e,d} = \frac{Ex_{0,d}}{Ex_{e,d}} \text{ for upstream interference}$$

$$FI_{e,d} = \frac{Ex_{e,0}}{Ex_{e,d}} \text{ for downstream antagonism}$$

The characteristic profiles of weak inhibition on logarithmic plots are better displayed with fold inhibition-1 than with fold inhibition.

The termination efficiency, TE, was calculated by

$$TE = \left(1 - \frac{FI_e(T) - 1}{FI_e(NT) - 1}\right) \times 100$$

FI_e denotes the fold inhibition of expression owing to the presence of estradiol. T and NT in the parentheses stand for the constructs with and without transcriptional terminator, respectively.

Model fitting

When the intergenic transcription was strong, the equilibrium competition model did not approximate well the full data set (Supplementary Figure S10), although it agreed well with the data obtained at high concentrations of doxycycline (Figure 2B and C). In such cases, the equation was fitted to only those data points that had a normalized expression higher than 0.4. This approach exposes how the remaining data points, obtained at lower doxycycline concentrations, deviate from the competition model. Subsequently, the competition model can be complemented parsimoniously.

To fit the non-equilibrium models to the experimental data, the concentration of the functionally active transcriptional activator, A_{UAS}, has to be extrapolated from the inducer (estradiol or doxycycline) concentration, ind, and the total activator concentration, A_{tot}.

$$A_{UAS} = A_{tot}\frac{ind}{K_{ind} + ind}$$

K_{ind} is a lumped equilibrium constant and represents the transport of the inducer across the cell membrane, and the binding of the inducer to the activator. Its fitted value depends also on the activity fluctuations of the inducer.

Supplementary information

Supplementary information is available at the *Molecular Systems Biology* website (www.nature.com/msb).

Acknowledgements

We thank Beatrice Blattmann and Simone Scherrer for technical help; Walter Schaffner, Bernhard Dichtl and Denise Hengartner (BUSS) for helpful discussions; and Reine Byun for reading the paper. This study was supported by the Swiss National Foundation and the UZH-URPP.

Conflict of interest

The authors declare that they have no conflict of interest.

References

Abarrategui I, Krangel MS (2007) Noncoding transcription controls downstream promoters to regulate T-cell receptor alpha recombination. *EMBO J* **26:** 4380–4390

Basu S, Gerchman Y, Collins CH, Arnold FH, Weiss R (2005) A synthetic multicellular system for programmed pattern formation. *Nature* **434:** 1130–1134

Becskei A, Kaufmann BB, van Oudenaarden A (2005) Contributions of low molecule number and chromosomal positioning to stochastic gene expression. *Nat Genet* **37:** 937–944

Bickel KS, Morris DR (2006) Role of the transcription activator Ste12p as a repressor of PRY3 expression. *Mol Cell Biol* **26:** 7901–7912

Bird AJ, Blankman E, Stillman DJ, Eide DJ, Winge DR (2004) The Zap1 transcriptional activator also acts as a repressor by binding downstream of the TATA box in ZRT2. *EMBO J* **23:** 1123–1132

Bird AJ, Gordon M, Eide DJ, Winge DR (2006) Repression of ADH1 and ADH3 during zinc deficiency by Zap1-induced intergenic RNA transcripts. *EMBO J* **25:** 5726–5734

Brent R, Ptashne M (1984) A bacterial repressor protein or a yeast transcriptional terminator can block upstream activation of a yeast gene. *Nature* **312:** 612–615

Buchler NE, Gerland U, Hwa T (2003) On schemes of combinatorial transcription logic. *Proc Natl Acad Sci USA* **100:** 5136–5141

Byrnes JK, Morris GP, Li WH (2006) Reorganization of adjacent gene relationships in yeast genomes by whole-genome duplication and gene deletion. *Mol Biol Evol* **23:** 1136–1143

Chiaromonte F, Miller W, Bouhassira EE (2003) Gene length and proximity to neighbors affect genome-wide expression levels. *Genome Res* **13:** 2602–2608

Cornish-Bowden A (2004) *Fundamentals of Enzyme Kinetics*. London: Portland Press

Cox III RS, Surette MG, Elowitz MB (2007) Programming gene expression with combinatorial promoters. *Mol Syst Biol* **3:** 145

De Freitas JM, Kim JH, Poynton H, Su T, Wintz H, Fox T, Holman P, Loguinov A, Keles S, van der Laan M, Vulpe C (2004) Exploratory and confirmatory gene expression profiling of mac1Delta. *J Biol Chem* **279:** 4450–4458

Galburt EA, Grill SW, Wiedmann A, Lubkowska L, Choy J, Nogales E, Kashlev M, Bustamante C (2007) Backtracking determines the force sensitivity of II RNAP in a factor-dependent manner. *Nature* **446:** 820–823

Hermsen R, Tans S, ten Wolde PR (2006) Transcriptional regulation by competing transcription factor modules. *PLoS Comput Biol* **2:** e164

Hongay CF, Grisafi PL, Galitski T, Fink GR (2006) Antisense transcription controls cell fate in *Saccharomyces cerevisiae*. *Cell* **127:** 735–745

Kaplan S, Bren A, Dekel E, Alon U (2008) The incoherent feed-forward loop can generate non-monotonic input functions for genes. *Mol Syst Biol* **4:** 203

Khaitovich P, Kelso J, Franz H, Visagie J, Giger T, Joerchel S, Petzold E, Green RE, Lachmann M, Paabo S (2006) Functionality of intergenic transcription: an evolutionary comparison. *PLoS Genet* **2:** e171

Lenasi T, Contreras X, Peterlin BM (2008) Transcriptional interference antagonizes proviral gene expression to promote HIV latency. *Cell Host Microbe* **4:** 123–133

Li Q, Johnston SA (2001) Are all DNA binding and transcription regulation by an activator physiologically relevant? *Mol Cell Biol* **21:** 2467–2474

Liao BY, Zhang J (2008) Coexpression of linked genes in mammalian genomes is generally disadvantageous. *Mol Biol Evol* **25:** 1555–1565

Louvion JF, Havaux-Copf B, Picard D (1993) Fusion of GAL4-VP16 to a steroid-binding domain provides a tool for gratuitous induction of galactose-responsive genes in yeast. *Gene* **131:** 129–134

Mangan S, Alon U (2003) Structure and function of the feed-forward loop network motif. *Proc Natl Acad Sci USA* **100:** 11980–11985

Martens JA, Laprade L, Winston F (2004) Intergenic transcription is required to repress the *Saccharomyces cerevisiae SER3* gene. *Nature* **429:** 571–574

Martens JA, Wu PY, Winston F (2005) Regulation of an intergenic transcript controls adjacent gene transcription in *Saccharomyces cerevisiae*. *Genes Dev* **19:** 2695–2704

Mosrin-Huaman C, Turnbough Jr CL, Rahmouni AR (2004) Translocation of *Escherichia coli* RNA polymerase against a protein roadblock *in vivo* highlights a passive sliding mechanism for transcript elongation. *Mol Microbiol* **51:** 1471–1481

Murphy KF, Balazsi G, Collins JJ (2007) Combinatorial promoter design for engineering noisy gene expression. *Proc Natl Acad Sci USA* **104:** 12726–12731

Neil H, Malabat C, d'Aubenton-Carafa Y, Xu Z, Steinmetz LM, Jacquier A (2009) Widespread bidirectional promoters are the major source of cryptic transcripts in yeast. *Nature* **457:** 1038–1042

Oehler S, Alberti S, Muller-Hill B (2006) Induction of the lac promoter in the absence of DNA loops and the stoichiometry of induction. *Nucleic Acids Res* **34:** 606–612

Prescott EM, Proudfoot NJ (2002) Transcriptional collision between convergent genes in budding yeast. *Proc Natl Acad Sci USA* **99:** 8796–8801

Ratna P, Scherrer S, Fleischli C, Becskei A (2009) Synergy of repression and silencing gradients along the chromosome. *J Mol Biol* **387:** 826–839

Sanchez L, Thieffry D (2003) Segmenting the fly embryo: a logical analysis of the pair-rule cross-regulatory module. *J Theor Biol* **224:** 517–537

Schmitt S, Prestel M, Paro R (2005) Intergenic transcription through a polycomb group response element counteracts silencing. *Genes Dev* **19:** 697–708

Shearwin KE, Callen BP, Egan JB (2005) Transcriptional interference—a crash course. *Trends Genet* **21:** 339–345

Sneppen K, Dodd IB, Shearwin KE, Palmer AC, Schubert RA, Callen BP, Egan JB (2005) A mathematical model for transcriptional interference by RNA polymerase traffic in *Escherichia coli*. *J Mol Biol* **346:** 399–409

Uhler JP, Hertel C, Svejstrup JQ (2007) A role for noncoding transcription in activation of the yeast *PHO5* gene. *Proc Natl Acad Sci USA* **104:** 8011–8016

Urlinger S, Baron U, Thellmann M, Hasan MT, Bujard H, Hillen W (2000) Exploring the sequence space for tetracycline-dependent transcriptional activators: novel mutations yield expanded range and sensitivity. *Proc Natl Acad Sci USA* **97:** 7963–7968

Valerius O, Brendel C, Duvel K, Braus GH (2002) Multiple factors prevent transcriptional interference at the yeast ARO4-HIS7 locus. *J Biol Chem* **277:** 21440–21445

Xu Z, Wei W, Gagneur J, Perocchi F, Clauder-Munster S, Camblong J, Guffanti E, Stutz F, Huber W, Steinmetz LM (2009) Bidirectional promoters generate pervasive transcription in yeast. *Nature* **457:** 1033–1037